Effect of Rail/Armature Geometry on Current Density Distribution and Inductance Gradient

Bok-ki Kim
Institute for Advanced Technology, The University of Texas at Austin, 4030-2 W. Braker Lane, Austin, TX 78759
Kwangwoon University, 447-1 Wolgye-dong, Nowon-gu, Seoul, 139-701, Korea

Kuo-Ta Hsieh
Institute for Advanced Technology, The University of Texas at Austin, 4030-2 W. Braker Lane, Austin, TX 78759

***Abstract*—The distribution of current in the conductors which is affected by the geometry of the armature and the velocity of the armature plays an important role in the performance of an electromagnetic launcher. In the early launching stage the current tends to flow on the outer surfaces of the conductors, resulting in high local current densities. Later in the launch, the tendency for current to concentrate on the surface is driven by the velocity skin effect. High current densities produce high local heating and, consequently, increased armature wear. This paper investigates the effects of rail/armature geometry on current density distribution and launcher inductance gradient (L′). Three geometrical parameters are used to characterize the railgun systems. These are the ratio of contact length to root length, relative position of contact leading edge to root trailing edge, and the ratio of rail overhang to the rail height. The distribution of current density and L′ for various configurations are compared.**

***Index Terms*—inductance gradient, railgun.**

I. Introduction

Various rail/armature configurations are used in railguns to achieve different performance benefits. A square bore railgun with rail overhang and a block or "C"-type armature geometry is widely used currently. The block armature is considered the simplest type, while the "C"-type armature is considered to be more practical in the sense of maintaining good sliding electric contact over the launch [1, 2, 3]. The armature plays an important role in an electromagnetic (EM) launcher system since railgun performance, particularly transition behavior, depends on armature design. In general, current density distribution over the armature is affected by a number of parameters such as the velocity of the moving armature, the armature geometry, rail overhang, and armature and rail materials.

Manuscript received May 1, 1998.
Bok-ki Kim, email: bkkim@daisy.kwangwoon.ac.kr, phone: 82-2-940-5254, fax: 82-2-917-1361.
Kuo-Ta Hsieh, email: kuota_hsieh@iat.utexas.edu, phone: 512-471-9060, fax: 512-471-9096.
This work was supported by the U.S. Army Research Laboratory (ARL) under contract DAAA 21-93-C-0101.

Due to the skin effect, the current tends to flow on the outer surfaces of the conductors during the early launch period, resulting in high local current densities. Later in the launch, the tendency for current to concentrate on the outer surface is driven by the velocity skin effect (VSE). High current densities produce high local heating that may increase armature wear, an important contribution to the transition phenomenon. Several techniques have been suggested for achieving more uniform distribution of current in railgun armatures. These include cladding or coating the rail and/or armature, multiple leaf armature, transposed wire armature, and other modifications to armature geometry [1, 2].

Long [1] has investigated the effects of electrical current and velocity on the performance of a railgun. In his dissertation, fundamental velocity limits based upon Joule heating for different rail/armature designs and materials was determined using a two-dimensional (2-D) finite element (FE) code. Yun and Price [3] perform three-dimensional (3-D) modeling for electromagnetic and structural analyses of electric gun and integrated launch package systems.

This paper investigates how the rail/armature geometry affects the current density distributions and L′ of the railgun system. The principal comparison is made for the normal component (J_x) of current density (A/m^2) distribution over the contact interface between the rail and the armature. The J_x distribution over the interface is significantly affected by the railgun geometry. In addition, L′ results from the 2-D analytical approach [4] are compared with those from three-dimensional numerical simulations. L′ represents the launcher inductance gradient — inductance per unit length (H/m).

Section II of the paper discusses the simulation set up for this numerical study. Section III describes simulation results depending on several geometrical parameters. The results of L′ calculated by 3-D simulations and a 2-D analytical approach are also discussed. Finally, Section IV summarizes the conclusions.

II. Simulation Set Up

The generic railgun geometry used in the investigation is shown in Fig. 1. The square bore of the railgun is 20 mm by 20 mm. Rails are assumed to be made of ETP copper and have a cross section 5 mm by 20 mm for the no overhang

models. The armature is made of 7071 T651 aluminum alloy with several shapes such as the block or "C"-type. Only a quarter of the model is constructed because of structural symmetry.

Four points are used to describe the geometry of the armature. These are the contact trailing edge (A), the contact leading edge (B), the root trailing edge (C), and the root leading edge (D), as shown in Fig. 1.

The root ratio (R_{root}) is defined as the ratio of contact length (L_c = B-A) to root length (L_r = D-C). The relative position between the contact leading edge (B) and the root trailing edge (C) is also an important parameter since it determines the lowest inductance path for current flow. To generate the different armature shapes for simulations, points A, B, and X are fixed and the line segments F-C and E-D are moved parallel to the rail to change the geometry. For example, moving the line F-C to F'-C' shown in Fig. 1 generates a model for a block armature.

A typical FE mesh of the "C"-shaped armature is illustrated in Fig. 2. A fine, non-uniform mesh is used near the trailing and leading edges of the armature and on the outer surface of the conductor region where high gradients of current density distribution usually occur.

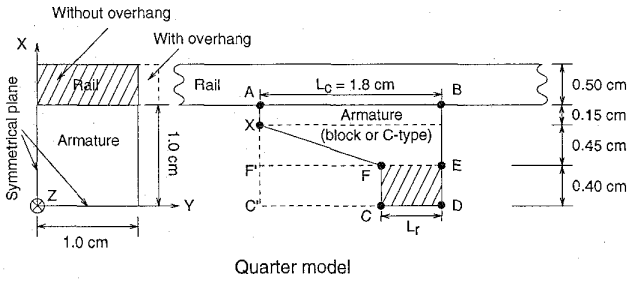

Fig. 1. A schematic armature and railgun with the important geometrical points identified. (A) Contact trailing edge, (B) Contact leading edge, (C) Root trailing edge, (D) Root leading edge.

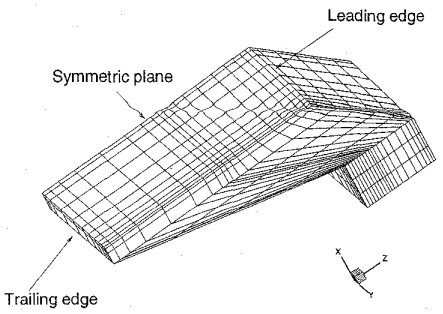

Fig. 2. A typical FE mesh of the detailed armature mesh for a "C"-shaped armature.

The 3-D EM FE code EMAP3D [5] is used for all numerical simulations. For the initial step, only stationary simulations with various rail/armature configurations are performed even though the current distribution at the armature/rail interface is significantly affected by the armature motion. A step input current of 5 x 10^4 A is applied at the breech end. Thermal effects are neglected. Perfect electrical contact between the rail and the armature is assumed. The calculated current distributions are compared at 0.25 ms, while the calculated L′ results are compared with Kerrisk's results at 10 ms since the Kerrisk's 2-D model assumes high frequency limit.

III. Simulation Results For Different Geometrical Parameters

Three different simulations for various geometrical parameters are performed to show the effects on current distributions and L′, which will be discussed in Subsection D.

A. Different Root Ratios (R_{root})

The first geometrical variation is to investigate the effect of the root area ratio on the current density distribution over the contact region. A side view of the armatures for different root area ratios are shown in Fig. 3. The contact and root leading edge position is fixed while the root position changes along the z-direction. In this set of variations the rails have zero overhang.

The calculated results in Fig. 4 show that, depending on the root trailing edge position, the high current density area on the interface moves forward along with the root trailing edge since the current path is determined by the lowest inductance path during a current transient. However, the highest current density still appears at the trailing edge of the armature.

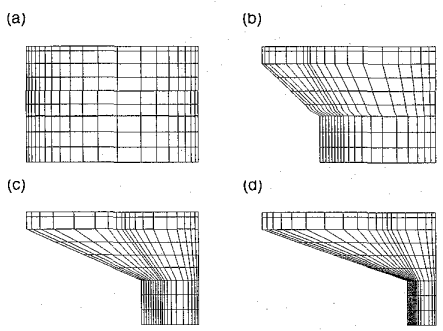

Fig. 3. Finite element mesh configurations of armatures for different root ratios. (a) R_{root} = 1, (b) R_{root} = 2/3, (c) R_{root} = 1/3, (d) R_{root} = 1/6.

With these results, it is reasonable to conclude that the position of the root trailing edge influences the current distribution over the contact interface.

B. Different "C"-type ratio (R_{ctype})

This section discusses how different "C"-type ratios affect current distribution. The "C"-type ratio represents the relative position of the root trailing edge of armature to the contact leading edge. From Fig. 1, the "C"-type ratio is defined as $R_{ctype} = (C - B) / L_r$. Various "C"-type armatures and their "C"-type ratios are shown in Fig. 5.

Numerical simulations show that the current distribution in a "C-type" armature is concentrated over the leading edge due to the lowest inductance path as shown in Fig. 6. As the "C"-type ratio increases, current is more concentrated toward the leading edge of the armature.

C. Different Rail Overhang Ratio R_{oh}

This section investigates how much the overhang ratio affects the current distribution over the rail/armature contact interface. Fig. 7 shows cross-sections of a railgun and armature for different overhang ratios. The overhang ratio represents the ratio of rail overhang to the armature height, which is $R_{oh} = L_{oh} / L_{arm}$ from Fig. 7 (b). L_{arm} is fixed with 1 cm. Three armature types are considered, a R_{root} type armature and two "C"-type armatures with $R_{ctype} = -1.0$ and $R_{ctype} = +0.0$ as shown in Fig. 5.

The numerical simulations for the block armature are shown in Fig. 8. The current distribution over the interface is affected by the overhang ratios. As the overhang ratio increases, magnetic flux linkage increases toward the leading edge of the armature and more of the current is distributed along the side and leading edge of the armature. Without overhang, very little current appears at leading edge and most of the current concentrates at the trailing edge.

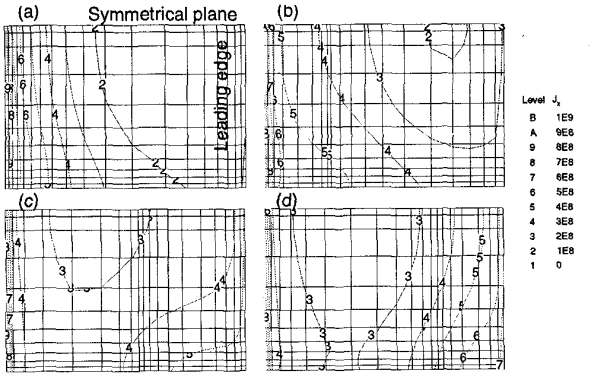

Fig. 4. Current density (J_x) distributions over the rail/armature contact interface for different root ratios. (a) R_{root} = 1, (b) R_{root} = 2/3, (c) R_{root} = 1/3, (d) R_{root} = 1/6.

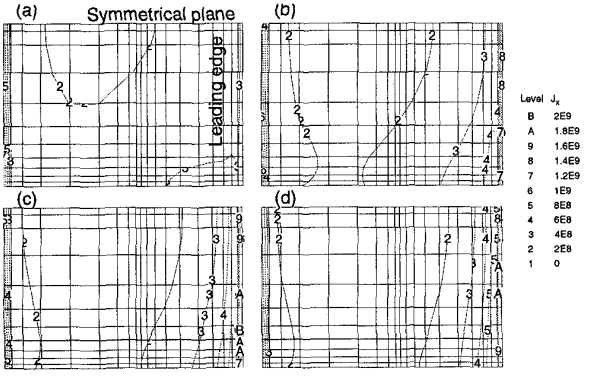

Fig. 6. Current density J_x distributions for different "C"-type ratios with R_{root} = 1/3, (a) $R_{ctype} = -1.0$, (b) $R_{ctype} = -0.5$, (c) $R_{ctype} = +0.0$, (d) $R_{ctype} = +0.5$.

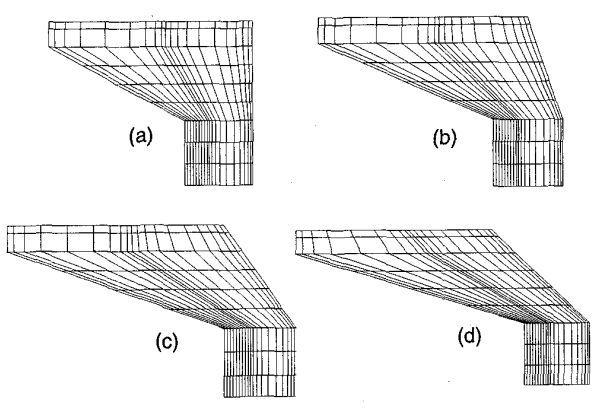

Fig. 5. Finite element mesh configurations for the different "C"-type ratios with a fixed R_{root} = 1/3. (a) $R_{ctype} = -1.0$, (b) $R_{ctype} = -0.5$, (c) $R_{ctype} = +0.0$, (d) $R_{ctype} = +0.5$.

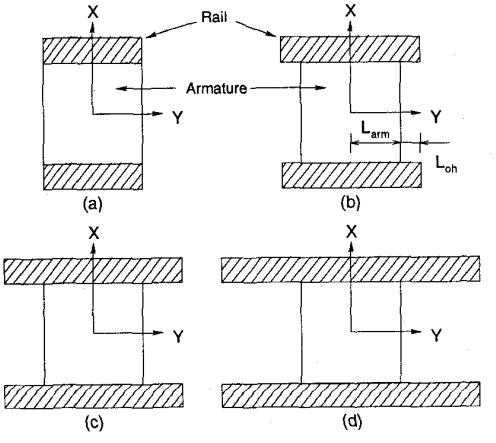

Fig. 7. Cross-sectional views for different overhang ratios. (a) R_{oh} = 0, (b) R_{oh} = 0.2, (c) R_{oh} = 0.4, (d) R_{oh} = 0.8, (L_{arm} = 1 cm).

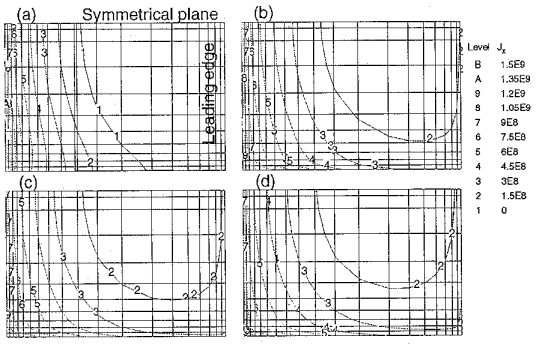

Fig. 8. Current density distributions (J_x) for different rail overhang ratios for a block armature. (a) $R_{oh} = 0$. (b) $R_{oh} = 0.2$. (c) $R_{oh} = 0.4$. (d) $R_{oh} = 0.8$.

The current distribution for the "C"-type armature shows the same behavior as the block armature case but it is not as apparent because the current is already concentrated toward the leading edge. The rail overhang makes the current move back from the leading edge.

D. Comparison of Inductance Gradient (L′)

The inductance gradient (L′) calculated from the 3-D numerical simulations is compared with the analytical solution from Kerrisk's 2-D model [4] in Table I. About 1 to 2.5% differences between the 3-D simulation and the 2-D analytical model are observed. In general, the L′ result of the 2-D computer simulation including the armature is higher than that of the 3-D simulation since the 2-D simulation assumes there is no flux in front of the armature. L′ for the 3-D simulation is calculated from the driving force relation [1, 5]:

$$F = J \times B = 1/2\, L'I^2. \qquad (1)$$

It is reasonable to conclude from Table I that L′ decreases as the current distribution moves to the front and sides of the armature as the overhang ratio increases. Tables I and II confirm the theoretical expectation that the dependence of L′ on "C"-type ratio is not significant.

TABLE I. COMPARISON OF L′ (μH/m) DUE TO THE RAIL OVERHANG BETWEEN THE 3-D NUMERICAL SIMULATIONS AT t = 0.25 ms AND A 2-D ANALYTICAL APPROACH OF KERRISK [4]

Overhang (%)	Kerrisk [4]	$R_{ctype} = -1.0$	$R_{ctype} = +0.0$
0	0.5278	0.5248	0.5224
20	0.4824	0.4904	0.4904
40	0.4447	0.4536	0.4528
80	0.3855	0.3960	0.3952

TABLE II. COMPARISON OF L′ (μH/m) OF "C"-TYPE ARMATURES WITHOUT RAIL OVERHANG AT t = 0.25 ms. (KERRISK'S VALUE IS 0.5278 μH.)

"C"-type		Root	
R_{ctype}	L′	R_{root}	L′
-1.0	0.5248	-	-
-0.5	0.5232	2/3	0.5272
+0.0	0.5224	1/3	0.5248
+0.5	0.5256	1/6	0.5208

IV. Conclusions

This paper investigates the effect of rail/armature geometry on the current density distribution for solid armatures at the rail/armature interface and L′ of the railgun system.

Three sets of 3-D finite element numerical simulations are performed for the various geometrical parameters. It is observed that the current density is significantly changed according to the overhang ratio, the root ratio, and the "C"-type ratio. Meanwhile, L′ results are closely related with the overhang ratio (actually rail geometry only), but not with the armature shape. In addition, the comparison of L′ results between the 2-D analytical approach and 3-D numerical simulation shows a reasonable agreement in the sense of high frequency limit.

It is concluded that the relative position between the contact leading edge and the root trailing edge is the most important geometrical parameter since it determines the lowest inductance path.

Acknowledgment

The authors wish to acknowledge computational support from the High Performance Computing Facility, The University of Texas at Austin.

References

[1] G. C. Long, "Fundamental limits to the velocity of solid armatures in railguns," The University of Texas at Austin, Dissertation, pp. 171, August 1987.

[2] R. A. Marshall, C. Persad, K. A. Jamison, and M. J. Matyac, "Observation of solid armature behavior," *IEEE Transactions on Magnetics*, vol. 31, no. 1, pp. 214-218, January 1995.

[3] J. J. Price and H. D. Yun, "Design and testing of integrated metal armature sabots for launch of armor penetrating projectiles from electric guns," *IEEE Transactions on Magnetics*, vol. 31, no. 1, pp. 219-223, January 1995.

[4] F. Kerrisk, "Current distribution and inductance calculation for railgun conductors," Los Alamos National Laboratory Report LA-9092-MS, October 1980.

[5] K. T. Hsieh, "A Lagrangian formulation for mechanically, thermally coupled electromagnetic diffusive processes with moving conductors," *IEEE Transactions on Magnetics*, vol. 31, no. 1, pp. 604-609, January 1995.